Biochemical and Structural Insights into Carbonic Anhydrase XII/ Fab6A10 Complex

Vincenzo Alterio[1,†], Markus Kellner[2,†], Davide Esposito[1], Friederike Liesche-Starnecker[3], Silvia Bua[4], Claudiu T. Supuran[4], Simona Maria Monti[1], Reinhard Zeidler[2,5] and Giuseppina De Simone[1]

*1 - **Istituto di Biostrutture e Bioimmagini,** CNR, Via Mezzocannone 16, Naples, 80134, Italy*
*2 - **Department of Gene Vectors,** Helmholtz Center for Environmental Health, Munich, Germany*
*3 - **School of Medicine,** Institute of Pathology, Department of Neuropathology, Technical University Munich, Munich, Germany*
*4 - **Dipartimento Neurofarba,** Sezione di Scienze Farmaceutiche e Nutraceutiche, UniversitàDegli Studi di Firenze, Via U. Schiff 6, Sesto Fiorentino, Florence, 50019, Italy*
*5 - **Department of Otorhinolaryngology,** Klinikum der Universität München, Munich, Germany*

***Correspondence to Giuseppina De Simone, Simona Maria Monti, and Reinhard Zeidler:** Reinhard Zeidler is to be contacted at: Department of Gene Vectors, Helmholtz Center for Environmental Health, Munich, Germany. marmonti@unina.it, zeidler@helmholtz-muenchen.de, gdesimon@unina.it*
https://doi.org/10.1016/j.jmb.2019.10.022

Abstract

6A10 is a CA XII inhibitory monoclonal antibody, which was demonstrated to reduce the growth of cancer cells *in vitro* and in a xenograft model of lung cancer. It was also shown to enhance chemosensitivity of multiresistant cancer cell lines and to significantly reduce the number of lung metastases in combination with doxorubicin in mice carrying human triple-negative breast cancer xenografts. Starting from these data, we report here on the development of the 6A10 antigen-binding fragment (Fab), termed Fab6A10, and its functional, biochemical, and structural characterization. *In vitro* binding and inhibition assays demonstrated that Fab6A10 selectively binds and inhibits CA XII, whereas immunohistochemistry experiments highlighted its capability to stain malignant glioma cells in contrast to the surrounding brain tissue. Finally, the crystallographic structure of CA XII/Fab6A10 complex provided insights into the inhibition mechanism of Fab6A10, showing that upon binding, it obstructs the substrate access to the enzyme active site and interacts with CA XII His64 freezing it in its *out* conformation. Altogether, these data indicate Fab6A10 as a new promising therapeutic tool against cancer.

Introduction

Human carbonic anhydrases (hCAs) represent a family of enzymes that catalyze the reversible hydration of CO_2 to HCO_3^- ions and protons [1,2]. There are 12 catalytically active isoforms known in humans (CAs I–IV, VA and VB, VI, VII, IX, XII–XIV) that differ with respect to tissue and organ distribution, as well as catalytic efficiency and cellular localization. Despite these differences, hCAs share a high level of three-dimensional similarity, a zinc ion in the active site, and the same two-step catalytic mechanism described by Eqs. (1) and (2) [1]:

$$EZn^{2+} - OH^- + CO_2 \rightleftarrows EZn^{2+} - HCO_3^- \overset{H_2O}{\rightleftarrows} EZn^{2+} - H_2O + HCO_3^- \quad (1)$$

$$EZn^{2+} - H_2O + B \rightleftarrows EZn^{2+} - OH^- + BH^+ \quad (2)$$

The first step of this mechanism involves the nucleophilic attack of a Zn^{2+}-bound hydroxide on a CO_2 molecule bound in a hydrophobic pocket within

Please cite this article as: V. Alterio, M. Kellner, D. Esposito, et al., Biochemical and Structural Insights into Carbonic Anhydrase XII/ Fab6A10 Complex, Journal of Molecular Biology, https://doi.org/10.1016/j.jmb.2019.10.022

the active site, with consequent formation of HCO_3^-, which is subsequently displaced by a water molecule with the generation of the catalytically inactive form of the enzyme EZn^{2+}-H_2O (Eq. (1)). The second step, which is rate-limiting, regenerates the Zn^{2+}-bound hydroxide through a proton transfer reaction from the Zn^{2+}-bound water molecule to the bulk solvent (Eq. (2); B indicates an exogenous proton acceptor from solvent) [1,3]. In most human isoforms, His64 residue, positioned in the middle of the active site cavity, assists this step by acting as a proton shuttle [4–6]. Indeed, His64 is generally observed in two different conformations, termed *in* and *out* [7–13]. In the *in* conformation, this histidine is orientated toward the interior of the active site to accept a proton from a network of water molecules that connects His64 to the zinc-bound water molecule, whereas in the *out* conformation it is orientated toward the external of the active site to deliver the proton to the bulk solvent (Fig. S1) [7–9]. Several studies suggested that the His64 conformational mobility is an essential requirement for proton transfer [3].

Catalyzing a simple yet fundamental reaction, human CAs are involved in many physiological processes; consequently, their abnormal expression levels and/or activities have been associated to different human diseases, including glaucoma, epileptic seizures, altitude illnesses, obesity, pain, and cancer [2]. For these reasons, CAs represent an interesting therapeutic target for the development of inhibitors or activators with biomedical applications [1].

Among the 12 catalytically active human isoforms, the two membrane-associated isoforms, hCA IX and hCA XII, have been shown to be overexpressed in many tumors and associated with cancer progression and metastases [14,15]. However, whereas hCA IX has been extensively characterized for drug design studies [16,17] which culminated in the progress of the sulfonamide inhibitor SLC-0111 and the monoclonal antibody RENCAREX® to clinical studies [18–23], hCA XII has been marginally investigated so far.

hCA XII is a transmembrane protein consisting of an extracellular N-terminal CA domain, a transmembrane (TM) region, and a small intracytoplasmatic (IC) tail containing potential phosphorylation sites [24]. Structural studies revealed for the catalytic domain a dimeric quaternary structure and a typical α-CA fold, characterized by a central twisted β-sheet surrounded by helical connections and additional β-strands [25]. The active site is located in a large, conical cavity, which spans from the protein surface to the center of the molecule and contains on its bottom the catalytic zinc ion coordinated by three conserved histidine residues [25].

Recently, a monoclonal antibody (mAb) towards CA XII, termed as 6A10, has been developed which is able to efficiently inhibit CA XII enzymatic activity *in vitro* [26] and in intact cells [27]. Notably, 6A10 reduces the growth of cancer cells *in vitro* and in a xenograft model of lung carcinoma, with a postulated mode of action directly dependent from inhibition of CA XII catalytic activity [27]. 6A10 was also shown to interfere with P-glycoprotein (P-GP) activity in chemoresistant cancer cell lines, resulting in enhanced chemosensitivity [28], and to significantly reduce the number of lung metastases in doxorubicin-treated mice, carrying human triple-negative breast cancer xenografts [28]. These data demonstrated that inhibition of CA XII by 6A10 could be effectively used to reduce chemoresistance of cancer cells and to interfere with the metastatic process in a clinical setting [28].

Due to the promising features of 6A10, a recombinant antigen-binding fragment (Fab) of this antibody, hereafter termed Fab6A10, has been developed. Indeed, the usage of antibody fragments has several advantages compared with full IgG monoclonal antibodies including a lower immunogenicity [29,30] and a faster penetration of tissues [31]. Here, we report an extensive biochemical and structural characterization of Fab6A10. Binding and inhibition assays demonstrated that Fab6A10 is highly specific toward CA XII, inhibiting its catalytic activity as the parental mAb 6A10. In addition, the crystallographic structure of the CA XII/Fab6A10 complex has been solved providing molecular insights into the inhibition mechanism of this Fab. Our data clearly indicate Fab6A10 as a new promising tool for the adjuvant treatment of different types of CA XII-positive cancer.

Results

Fab6A10 production, affinity, and specific binding to hCA XII

The variable immunoglobulin sequences of 6A10 were obtained by rapid amplification of cDNA ends (RACE)-PCR and fused to the constant Fab part of a hIgG1 molecule by gene synthesis. Fab6A10 was produced in CHO cells stably transfected with expression plasmids encoding the heavy and light Ig gene fragments and subsequently purified from the supernatant by affinity chromatography.

The capability of Fab6A10 to bind CA XII-positive human A549 lung cancer cells was investigated by flow cytometry incubating cells with serial dilutions of Fab6A10 (Fig. 1A and B). A concentration-dependent increase of the fluorescent signal was observed, and a K_d value of 3.4 nM was assessed (Fig. 1B and Table S1).

The specificity of Fab6A10 was assessed by comparing its binding to CA XII-positive parental ASPC1 pancreatic cancer cells with a CA XII-negative knockout subclone. Although binding of Fab6A10 to parental ASPC1 cells was clearly detectable (Fig. 1C), the CA XII-negative subclone was completely negative (Fig. 1D).

Please cite this article as: V. Alterio, M. Kellner, D. Esposito, et al., Biochemical and Structural Insights into Carbonic Anhydrase XII/Fab6A10 Complex, Journal of Molecular Biology, https://doi.org/10.1016/j.jmb.2019.10.022

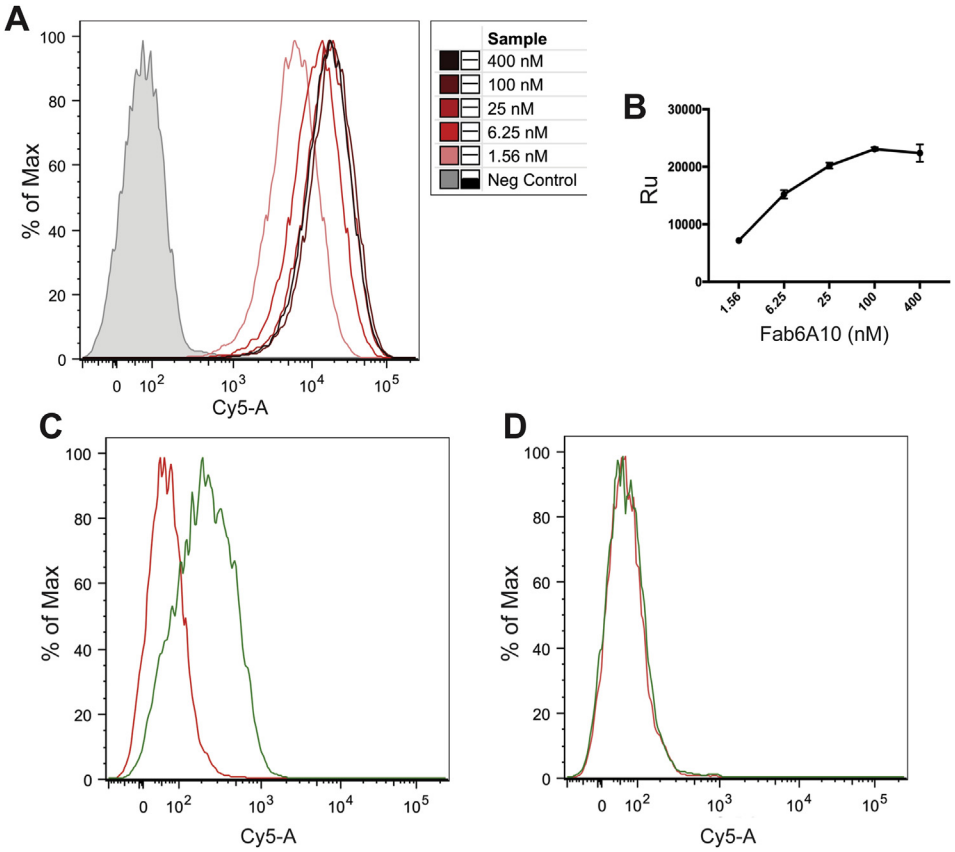

Fig. 1. Affinity and specific binding of Fab6A10 to CA XII. (**A, B**) CA XII positive A549 cells were incubated with serial dilutions of Fab6A10 (1.56 nM−400 nM). Cells were subsequently stained with a secondary antibody (donkey antihuman Alexa467) and measured by flow cytometry (Cy5 channel). Image shows original flow cytometric histograms (**A**) and binding curve in diagram (**B**). (**C**, **D**) Specificity of Fab6A10 to CA XII. Fab6A10 (green) and an isotype control antibody (red) were incubated with CA XII-positive cell lines (ASPC1 wt) (**C**) and CA XII-negative cell lines (ASPC1 k.o) (**D**). Cells were stained with a secondary antibody (antihuman Alexa647) and measured by flow cytometry.

To provide further evidence of the specific binding between Fab6A10 and CA XII, surface plasmon resonance (SPR) experiments were carried out using the two purified recombinant proteins, and results were compared with those obtained using mAb 6A10. In details, either Fab6A10 or mAb 6A10 were amine-coupled to the sensor chip and subsequently incubated with serial dilutions of recombinant human CA XII. A K_D of 12.8 nM was measured for the Fab compared with a K_D of 5.8 nM for the entire antibody (Fig. S2 and Table S1). This difference is likely due to the monovalent character of the Fab compared with the bivalent nature of full-length 6A10 [32].

Finally, the binding capability of Fab6A10 to primary tumor tissues was evaluated by immunohistochemistry. Here again, experiments were carried out with mAb 6A10 for comparison. In detail, human glioblastoma and astrocytoma, both reported to express high levels of CA XII [33], stained positive with 6A10 (Fig. 2A and B). Similar results were obtained with Fab6A10 (Fig. 2C). In the infiltration zone, only the tumor cells show a distinct reaction in contrast to the negative infiltrated tissue (Fig. 2D). Taken together, these data demonstrate the capacity of Fab6A10 to bind CA XII *in vitro*.

Inhibition properties of Fab6A10 on hCA XII catalytic activity

Because mAb 6A10 was reported to inhibit *in vitro* CA XII enzymatic activity [26], the inhibitory effect of Fab6A10 on both the esterase and the CO_2 hydration activity of CA XII was evaluated here. Esterase inhibition assays (Fig. S3) showed that Fab6A10 likewise its parental antibody is an efficient inhibitor of this activity.

CO_2 hydration inhibition assays (Table 1) showed that Fab6A10 blocks also this activity very efficiently with a K_I of 6.6 nM, comparable with that of the original, full-length antibody (K_I of 6A10 = 3.1 nM) [26]. Interestingly, Fab6A10 does not inhibit the off-target isoforms CA I, CA II, and CA IX.

Please cite this article as: V. Alterio, M. Kellner, D. Esposito, et al., Biochemical and Structural Insights into Carbonic Anhydrase XII/Fab6A10 Complex, Journal of Molecular Biology, https://doi.org/10.1016/j.jmb.2019.10.022

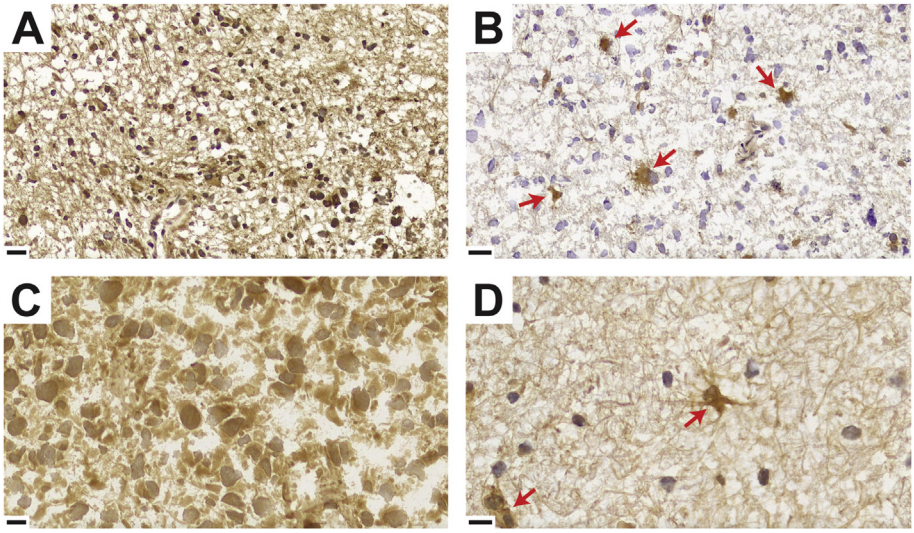

Fig. 2. Frozen sections of human tissues immunostained with either mAb 6A10 (A, B) or Fab6A10 (C, D). Brown staining shows positivity of cells; negative cells are blue through counterstaining with hematoxylin. (**A**) Glioblastoma (highly malignant brain tumor). Strong staining of the tumor cells (scale bar: 20 μm). (**B**) Infiltration zone of a diffuse astrocytoma (low-grade brain tumor). Positive staining of infiltrating tumor cells (red arrows), surrounded by CA XII negative brain tissue (scale bar: 20 μm). (**C**) Glioblastoma. Strong staining of the tumor cells (scale bar: 10 μm). (**D**) Infiltration zone of a glioblastoma. Positive staining of infiltrating tumor cells (red arrows), surrounded by CA XII negative infiltrated brain tissue (scale bar: 10 μm).

Table 1. Inhibition data of hCA I, II, IX, and XII with Fab6A10. Inhibition data of the standard inhibitor acetazolamide (AAZ) are also reported for comparison.

Compound	K_I[a] (nM)			
	hCA I	hCA II	hCA IX	hCA XII
Fab6A10	>10000	>10000	>1000	6.6 ± 0.12
AAZ[b]	250	12.5	25	5.7

[a] Mean from three different assays, by a stopped flow technique.
[b] Data are taken from Battke et al.[26].

Biochemical and structural characterization of CA XII/Fab6A10 complex

A detailed biochemical and structural characterization of the complex formed by Fab6A10 and the CA XII catalytic domain was undertaken to elucidate the molecular basis of CA XII binding and inhibition by Fab6A10.

Before complex preparation, the oligomerization state of the recombinant CA XII was assessed by light scattering analysis showing that in our experimental conditions, differently from what reported by Whittington and coworkers [25], the protein exists as a monomer of 31 KDa (Fig. S4, red line). Concurrently, also Fab6A10 alone was investigated by light scattering, eluting as a monomer of 48 KDa (Fig. S4, green line). Complex formation was carried out by incubating CA XII and Fab6A10 in a 1:1 M ratio at 20 °C for 18 h and further purifying it by size exclusion chromatography in order to remove any excess of uncomplexed proteins. As attended, the complex eluted as a unique peak with a molar mass of 79 KDa as shown by SEC-MALS-QELS (Fig. S4, blue line).

Crystals of the CA XII/Fab6A10 purified complex were obtained by the hanging drop method using ammonium sulfate as precipitant. They belonged to the I222 space group and diffracted to 2.8 Å resolution (Table 2). The structure was solved by molecular replacement using the crystallographic coordinates of CA XII in complex with a benzenesulfonamide inhibitor (PDB code 4WW8) [34] and the Fab of the antibody 13G5 (PDB code 3FO0) [35] as starting models, and refined to R_{work} and R_{free} values of 20.3% and 23.0%, respectively (see Table 2). The asymmetric unit contained two copies of the complex, which were refined with NCS restraints. The final model included for each complex residues from 3 to 262 of CA XII, residues 1-127 and 134-215 of the Fab heavy chain, and residues from 1 to 213 of the Fab light chain.

Please cite this article as: V. Alterio, M. Kellner, D. Esposito, et al., Biochemical and Structural Insights into Carbonic Anhydrase XII/Fab6A10 Complex, Journal of Molecular Biology, https://doi.org/10.1016/j.jmb.2019.10.022

Table 2. Data collection and refinement statistics for hCA XII/Fab6A10 complex. Values in parentheses refer to the highest resolution shell (2.85−2.80 Å).

Crystal parameters	
Space group	I222
a (Å)	77.3
b (Å)	222.2
c (Å)	267.0
Data collection statistics	
Resolution (Å)	49.6−2.8
Temperature (K)	100
Total reflections	272450
Unique reflections	56400
Completeness (%)	98.1 (91.8)
$<I>/<\sigma(I)>$	11.4 (2.0)
Redundancy	4.8 (2.5)
R_{merge} [a]	0.09 (0.49)
R_{meas} [a]	0.10 (0.61)
R_{pim} [a]	0.04 (0.36)
Refinement statistics	
Resolution (Å)	49.6−2.8
R_{work} [b] (%)	20.3
R_{free} [b] (%)	23.0
r.m.s.d. from ideal geometry:	
Bond lengths (Å)	0.008
Bond angles (°)	1.3
Number of protein atoms	10790
Number of water molecules	23
Number of ligand atoms	8
Average B factor (Å^2)	
All atoms	36.4
Protein atoms	36.5
Water molecules	18.7
Ligand atoms	25.5

[a] $R_{merge} = \Sigma_{hkl}\Sigma_i|I_i(hkl)-<I(hkl)>|/\Sigma_{hkl}\Sigma_i I_i(hkl)$; $R_{meas} = \Sigma_{hkl}\{n(hkl)/[n(hkl)-1]\}^{1/2}\Sigma_i|I_i(hkl)-<I(hkl)>|/\Sigma_{hkl}\Sigma_i I_i(hkl)$; $R_{pim} = \Sigma_{hkl}\{1/[n(hkl)-1]\}^{1/2}\Sigma_i|I_i(hkl)-<I(hkl)>|/\Sigma_{hkl}\Sigma_i I_i(hkl)$, where $I_i(hkl)$ is the intensity of an observation and $<I(hkl)>$ is the mean value for its unique reflection; summations are over all "n" reflections.

[b] $R_{work} = \Sigma_h||F_o(h)|-|F_c(h)||/\Sigma_h|F_o(h)|$, where F_o and F_c are the observed and calculated structure-factor amplitudes, respectively. R_{free} was calculated with 2.2% of the data excluded from the refinement.

The two complexes in the asymmetric unit revealed only minor differences, with an r.m.s.d for the superposition of the corresponding Cα of only 0.3 Å. For this reason, only one complex was arbitrarily chosen for the following discussion.

Analysis of the complex structure (Fig. 3) revealed that both the heavy and light chains of the Fab are involved in the binding to CA XII, contributing to 77% and 23%, respectively, of the buried surface area of the complex which is of about 1100 Å^2 on each side of interaction. A total of 11 potential hydrogen bonds (Table S2), four salt bridges (Table S3), and a large number of van der Waals contacts stabilize the binding.

Fab6A10 binds CA XII utilizing all complementarity-determining regions (CDRs) (H1, H2, H3, L1, L2, and L3) (Fig. S5). However, whereas L1, L2, and L3 interact with a protein region adjacent to the active site cleft, H1, H2, and H3 strongly interact with the rim of the catalytic cavity, acting as a plug on it (Fig. 3B and C). H3 is also able to penetrate in the upper side of the cavity, with residue Tyr98 at only 6.5 Å from the catalytic zinc ion (Fig. 3D). Interestingly, Fab6A10 does not interact directly with the three histidines coordinating the catalytic zinc ion (His94, His96, and His119), the gatekeeper residues Thr199 and Glu106, and the catalytic zinc ion, but a salt bridge interaction is observed between Asp54 of the Fab H2 loop and CA XII His64 (Fig. 3A). This interaction freezes His64 in its *out* conformation, thus not allowing conformational flexibility necessary for its action as proton shuttle (see Introduction) [3].

The structural superposition of the unbound CA XII with the same enzyme in complex with Fab reveals that the binding of Fab6A10 to the enzyme does not cause any rearrangement either in the backbone or in the conformation of the residues within the active site cavity (Fig. S6). Interestingly, also in the unbound hCA XII, His64 is in *out* conformation, but it is not forced in this position by any strong interaction as it happens for CA XII His64 in complex with Fab.

Finally, because binding and inhibition experiments demonstrated that FabA610 is very specific for CA XII, a comparison between CA XII and the other isoforms here evaluated (hCA I, hCA II, and hCA IX) was carried out to clarify the molecular basis of this high specificity. In particular, a structure-based sequence alignment was performed showing that the majority of CA XII residues involved in Fab binding are not conserved among the four isozymes (Fig. S7). Indeed, as described earlier, Fab6A10 binds the whole rim of the active site cavity, which is the most variable active site region among all hCAs as reported in literature [1,18,36−38].

Discussion

Differently to CA IX, whose expression mainly occurs in hypoxic tumors[14], CA XII beyond being overexpressed in various human tumors such as RCC [24], breast [39,40], colorectal [41,42], gastrointestinal [41], ovarian [43], and pancreatic [44] carcinoma and brain [33,45], is also present in several normal tissues [46]. However, the participation of CA XII into the extracellular acidification and maintenance of a more alkaline intracellular pH in hypoxic tumor cells [47] make this enzyme relevant to tumor research. In particular, the evidence that CA IX and CA XII knockout gives a remarkable reduction of xenograft tumor volume compared with knockout of CA IX alone [47], and that the simultaneous silencing of *ca9* and *ca12* combined with radiotherapy strongly decreased LS174Tr tumor progression *in vivo* [48], highlights how inhibition of both the proteins in tumors can have

Please cite this article as: V. Alterio, M. Kellner, D. Esposito, et al., Biochemical and Structural Insights into Carbonic Anhydrase XII/Fab6A10 Complex, Journal of Molecular Biology, https://doi.org/10.1016/j.jmb.2019.10.022

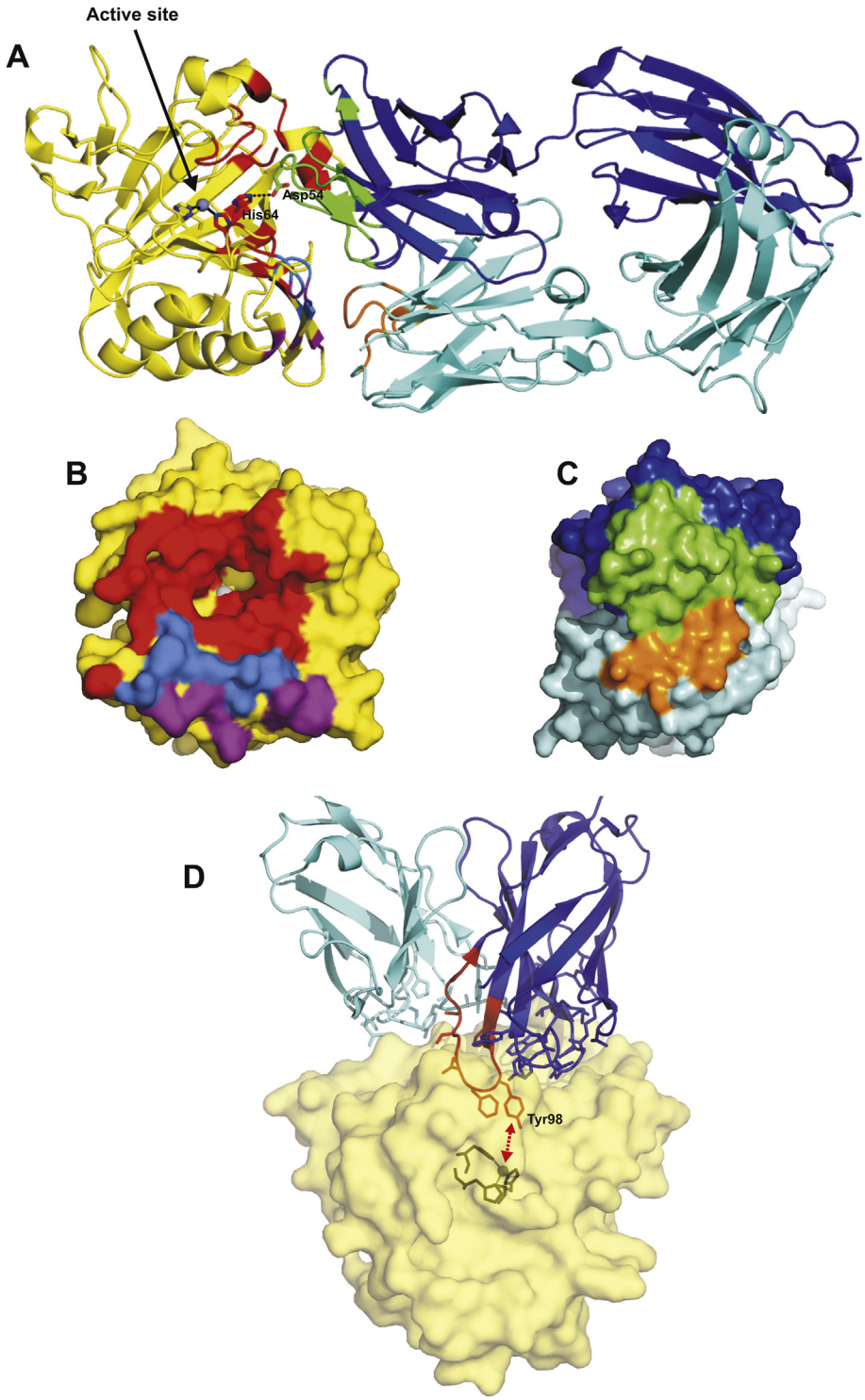

Fig. 3. Fab6A10/CA XII complex structure. (A) Ribbon representation. Fab6A10 is reported in blue (heavy chain) and cyan (light chain), whereas CA XII is reported in yellow. The CA XII zinc ion and its coordinating histidines are shown to indicate the position of the active site. hCA XII residues buried at the interface with Fab6A10 heavy chain and light chain are reported in red and violet, respectively, whereas those at interface with both chains are in light blue. Fab6A10 residues buried at complex interface are green (heavy chain) or orange (light chain). **(B, C)** Fab6A10/CA XII epitope and paratope as open-book representation: (**B)** Epitope of Fab6A10 on CA XII. Color code is as in **(A)**. The zinc ion at the bottom of the active site cavity is shown as a gray sphere. It is evident that the residues of CA XII at the interface with Fab6A10 heavy chain (residues in red) outline the whole rim of the active site cavity. **(C)** CA XII contact region on Fab6A10. Color code is

Please cite this article as: V. Alterio, M. Kellner, D. Esposito, et al., Biochemical and Structural Insights into Carbonic Anhydrase XII/Fab6A10 Complex, Journal of Molecular Biology, https://doi.org/10.1016/j.jmb.2019.10.022

a great antineoplastic potential [49]. Nevertheless, differently from CA IX, only few molecules specifically targeting CA XII have been developed and preclinically investigated so far [26–28,49]. Among these molecules, mAb 6A10 is one of the most promising [26–28].

Recent progress in the field of antibody engineering has allowed the development of Fabs as an interesting alternative to mAbs because they are easier to produce and purify, are less immunogenic, and show better tissue penetration and reduced toxicity [50]. Thus, based on these considerations and on the very encouraging results described for 6A10, in this paper, we reported on the development of Fab6A10 and its functional, biochemical, and structural characterization. We demonstrated the capability of Fab6A10 to bind selectively CA XII *in vitro*, to stain immunohistochemically malignant glioma cells in contrast to the surrounding infiltrated brain tissue, and to inhibit human CA XII. The obtained structural data are in agreement with these findings. Indeed, the crystallographic structure of the Fab6A10/CA XII complex showed that Fab6A10 strongly binds CA XII by interacting with the rim of the active site cavity, which is the least conserved active site region among all the human CA isoforms, thus explaining its strong specificity towards CA XII. Moreover, both the occlusion of the active site entrance and the limited conformational flexibility of His64 observed in the complex structure concur to the high inhibitory properties of Fab6A10. Interestingly, both mechanisms of inhibition have been described for small molecule CA inhibitors [38]. In particular, the occlusion of the enzyme active site is the mechanism utilized by coumarins, a class of small molecules acting as isoform-selective CA inhibitors [51,52], whereas some carboxylic acid derivatives have been reported to inhibit CAs by freezing His64 in its *out* conformation [53]. It is worth noting that to date only few other antibodies against CA XII and CA IX have been shown to inhibit enzyme catalytic activity [54–57], and that the inhibition mechanism has not been clarified in any of these.

Altogether, these data highlight that Fab6A10 retains all the features of the parental 6A10 antibody, turning it into an attractive candidate for various clinical applications. It is also important to highlight that the knowledge of the CA XII/Fab6A10 structure allows for the design of small molecules, which could act as CA XII selective inhibitors. Further studies are currently underway in our lab to investigate this topic.

Material and Methods

Preparation of the Fab6A10

Variable sequences of heavy (H) and light (L) chain of the 6A10 antibody were obtained by rapid amplification of cDNA ends (RACE; Kit by Invitrogen). For this, original rat-hybridoma cell lines were harvested (10^7) and the total RNA was isolated by phenol/chloroform and isopropanol precipitation. Subsequently, the RACE protocol was processed, beginning with cDNA synthesis, using isotype-specific primers (rat IgG2: ACAAGGATTGCATTCCCTTGG, Rat kappa: CTCATTCCTGTTGAAGCTCTTGACGAC). After cDNA purification by SNAP columns, a polyC-tail was added to the strands by a terminal deoxyribonucleotidyltransferase (TdT). Finally, a PCR was conducted with the cDNA template to obtain amplified variable sequences (primer: UAP from kit as fwd primer, and CTACTAGCATGCTCGAGCTCAATTTTCTTGTCCACCTTGGTGC as HC reverse or CTACTAGCATGCTCGAGCTCATTCCTGTTGAAGCTCTTGACGACGGG as LC reverse primer, respectively). The products were sequenced to elucidate the sequence of the variable parts of the 6A10 antibody. Then, a fused construct of the variable sequences, a secretion signal (IL-2), and the hIgG1-kappa constant part from the Fab site was synthesized (GenScript).

The sequences were subcloned into a pHIT basis vector (established by Fraunhofer Institute for Toxicology and Experimental Medicine) and transfected into CHO Hit cells (established by Fraunhofer Institute for Toxicology and Experimental Medicine). The Fab6A10 was purified on a CaptureSelect kappaXL column (GE Life Science). Elution of bound Fab was performed at pH = 5.0 as described in the manufacturer's instructions. Fab was eventually dialyzed against PBS and concentrated by Amicon-Ultra centrifugation filter units (Millipore).

Flow cytometry

Cells were harvested and incubated with Fab6A10 followed by incubation with a donkey anti-human IgG secondary antibody labeled with Alexa467. Cells were analyzed on a BD FACS Canto™ cytometer and analyzed with FlowJo 9 (FlowJo, LLC). Further data analysis and K_d determination was performed by GraphPad Prism 7.

Production of recombinant CA XII catalytic domain

DNA-sequence of CA XII catalytic domain was synthesized by GenScriptTM including a C-terminal His-tag and delivered in a pUC57 vector plasmid. The sequence was recloned into a pETM13 vector by using the restriction sites

as in **(A)**. **(D)** Detail of the CA XII/Fab6A10 complex. Fab6A10 is reported in blue (heavy chain) and cyan (light chain), whereas CA XII is reported in yellow. Fab6A10 residues buried at complex interface and CA XII zinc ion with the three coordinating histidines are shown in stick representation. H3 is colored in red. The close position of Tyr98 to the Zn^{2+} ion is highlighted.

Please cite this article as: V. Alterio, M. Kellner, D. Esposito, et al., Biochemical and Structural Insights into Carbonic Anhydrase XII/Fab6A10 Complex, Journal of Molecular Biology, https://doi.org/10.1016/j.jmb.2019.10.022

XbaI (5′) and HindIII (3′). The plasmid was transformed into *Escherichia coli* Rosetta (DE3). Bacteria were grown in an autoinduction medium [58] to an OD_{600} of 1.0 as a preculture, and subsequently diluted to an OD_{600} of 0.1 for final culture. Bacteria were grown to an OD_{600} of 2–5, harvested by centrifugation, resuspended in lysis buffer (50 mM sodium phosphate, 300 mM sodium chloride, 20 mM imidazole, 1 mg/mL lysozyme, pH 8.0) and incubated on Agarose-NTA-beads overnight. The beads were washed three times with wash buffers containing increasing imidazole content (50 mM sodium phosphate pH 8.0, 300 mM sodium chloride, 20/50/100 mM imidazole). Finally, CA XII was eluted with buffer containing 500 mM imidazole and dialyzed against 1× PBS.

Surface plasmon resonance

The ligand, here represented by Fab6A10 or mAb 6A10, was immobilized on a CM5 sensor chip (GE LifeSciences) by amine-coupling using a Biacore 3000™ according to the manufacturer's instructions. Conditions: 10 μg/mL ligand, solved in 10 mM sodium acetate, pH 4.5; 0.05 M N-hydroxysuccinimide (NHS), 0.02 M 1-ethyl-3-(3-dimethyl- aminopropyl) carbodiimide (EDC); washing solution 1 M ethanolamine. Subsequently, the analyte, represented by recombinant CA XII, was applied to the chip using different concentrations such as 5, 10, 50, 100 nM (each in duplicates) to perform a kinetic analysis. 4 M $MgCl_2$ served as regeneration solution. K_D values were calculated by the BIAevaluation software.

Immunohistochemistry

For CA XII immunohistochemistry, 8-μm-thick frozen sections were cut and fixed in Delaunay for 1 min. After that, pretreatment with H_2O_2 and blocking with normal horse serum at room temperature for 30 min followed. mAb 6A10 was incubated overnight at 4 °C in a dilution of 1:100, followed by incubation of biotinylated secondary anti-rabbit IgG antibody (Vector Laboratories, USA) in a dilution of 1:400 for 30 min. ABC-reagent (Vector Laboratories, USA) was applied for 30 min, followed by diaminobenzidine (DAB)-reagent (Dako, USA). For the immunostaining with Fab6A10, H_2O_2 incubation and blocking with normal horse serum was conducted, followed by incubation with Fab6A10 overnight at 4 °C in a dilution of 1:20.31A4/peroxidase (a kind gift of R. Feederle, Munich), which is a 6A10-specific antibody raised in mice, was used as a secondary antibody to specifically detect the Fab fragment. 31A4 was incubated for 1 h at room temperature in a dilution of 1:100 followed and developed with DAB-reagent (Dako, USA). For both immunohistochemical stainings, counterstaining with hematoxylin was conducted. For quality insurance, human kidney tissue served as positive control.

Staining specificity was evaluated by two neuropathologists. Slides were digitalized with PathoZoom Scan software (Smart in Media, Cologne, Germany). Images were taken with PathoZoom (Smart in Media, Cologne, Germany). For imaging, areas of highest staining quality with regard to tissue integrity were chosen.

Inhibition assays

Recombinant hCA XII (20 μg/mL) was incubated with either 6A10 mAb, Fab6A10 (each 1 μM), acetazolamide (50 μM) or left blank with only assay buffer (12.5 mM Tris, 75 mM NaCl, pH 7.5) for 1 h. 4-nitrophenylacetate (2 mM dissolved in acetone) was added and incubated for 90 min at 37 °C to generate an activity-dependent color shift, which was measured by ClarioStar® (BMG Labtech, Ortenburg, Germany) at 405 nm.

An SX.18V-R Applied Photophysics (Oxford, UK) stopped-flow instrument was used to assay the inhibition of human CA I, II, IX, and XII [59]. 0.2 mM Phenol Red was used as an indicator, working at an absorbance maximum of 557 nm, with 10 mM Hepes (pH 7.4) as a buffer, 0.1 M Na_2SO_4 or $NaClO_4$ (for maintaining constant the ionic strength; these anions are not inhibitory in the used concentration), following the CA-catalyzed CO_2 hydration reaction for a period of 5–10 s. Saturated CO_2 solutions in water at 25 °C were used as substrate. Stock solution of Fab was diluted up to 0.01 nM with the assay buffer. At least seven different inhibitor concentrations have been used for measuring the inhibition constant. Inhibitor (I) and enzyme (E) solutions were preincubated together for 1 h at 4 °C before assay, to allow for the formation of the E-I complex. Triplicate experiments were done for each inhibitor concentration, and the values reported in this paper are the mean of such results. The inhibition constants were obtained by nonlinear least squares methods using the Cheng-Prusoff equation, as reported earlier [60] and represent the mean from at least three different determinations. All CA isozymes used here were recombinant proteins obtained as reported earlier by our groups [60–63].

Complex formation and analysis

Recombinant CA XII catalytic domain, containing the C-terminal His-tag, was incubated with Fab6A10, previously purified by FPLC (GE Healthcare) using a Superdex 75 size exclusion chromatography column in 30 mM Tris, 150 mM NaCl, pH 8.0. CA XII/Fab6A10 complex was obtained incubating CA XII:Fab6A10 in 1:1 M ratio for 18 h at 20 °C. The complex was finally purified by Superdex 200 in 30 mM Tris, 150 mM NaCl, pH 8.0.

Quaternary structure investigations on CA XII, Fab6A10, and CA XII/Fab6A10 complex were performed by SEC-MALS-QELS (size exclusion chromatography—multiangle light scattering—quasi elastic light scattering) as previously reported [64,65]. In particular, analyses were carried out loading 50 μL of 2.0 mg/mL Fab6A10, 50 μL of 3.9 mg/mL CA XII, and 50 μL of 2.0 mg/mL CA XII/Fab6A10 complex on a Superdex 75 or 200 column (GE Healthcare), equilibrated in 30 mM Tris, 150 mM NaCl, pH 8.0 and connected to FPLC ÅKTA, coupled to a light scattering detector (mini-DAWN TREOS, Wyatt Technology) and a refractive index detector (Shodex RI-101). Data were analyzed using the program ASTRA 5.3.4.14 (Wyatt Technology Corporation).

Please cite this article as: V. Alterio, M. Kellner, D. Esposito, et al., Biochemical and Structural Insights into Carbonic Anhydrase XII/Fab6A10 Complex, Journal of Molecular Biology, https://doi.org/10.1016/j.jmb.2019.10.022

Cocrystallization of CA XII/Fab6A10 complex and structure determination

CA XII/Fab6A10 complex was crystallized at 293 K using the hanging drop vapor diffusion technique. Drops were prepared by mixing 1 μL of complex solution (5 mg/mL in 30 mM Tris-HCl, pH 8.0, 150 mM NaCl) with 1 μL of precipitant solution (1.5 M ammonium sulfate, 0.1 M sodium acetate, pH 5.5, 0.02 M $CdCl_2$), and equilibrated over a well containing 1 mL of precipitant solution. Diffraction data were collected to 2.8 Å resolution, in-house at 100 K, using a Rigaku MicroMax-007 HF generator producing Cu Kα radiation and equipped with a Saturn 944 CCD detector. Before cryogenic freezing, crystals were transferred to the precipitant solution with the addition of 20% (w/v) glycerol. Data were processed using the HKL2000 software package [66]. The crystals belonged to the space group I222 with unit cell dimensions of $a = 77.3$ Å, $b = 222.2$ Å, $c = 267.0$ Å. The Matthews coefficient ($V_M = 3.6$ Å^3/Da) indicated that the crystallographic asymmetric unit contained two CA XII/Fab6A10 complexes according to a solvent content of 66%. Data collection statistics are reported in Table 2.

The structure of CA XII/Fab6A10 complex was solved by molecular replacement technique using the program AMoRe [67], and the crystallographic structure of hCA XII (PDB code 4WW8) [34] and the Fab portion of the antibody 13G5 (PDB code 3FO0) [35] as model templates. The first cycles of structure refinement were carried out with CNS [68,69], using twofold NCS-restraints and an energy barrier of 300 kcal mol^{-1} Å^2. After R_{work} and R_{free} reached 23.2% and 25.3%, respectively, the noncrystallographic symmetry (NCS) restraints were reduced to 150 kcal mol^{-1} Å^2. Further cycles of restrained refinement were carried out using Refmac5 [70] to produce the final model with crystallographic R_{work} and R_{free} values (in the 49.6–2.8 Å resolution range) of 20.3% and 23.0%, respectively. Local NCS restraints, automatically generated by Refmac, were used in the refinement. Test set reflections were selected in thin shells with the program DATAMAN [71]. Model building was performed with the program O [72]. Data refinement statistics are summarized in Table 2. For the analysis of CA XII/Fab6A10 complex interactions, h-bonds, salt bridges, and buried residues have been determined by PISA [73], considering a distance between the heavy atoms (donor and acceptor) less than 3.5 Å and 4 Å for h-bonds and salt bridges, respectively.

Accession numbers

Coordinates and structure factors of the CA XII/Fab6A10 complex have been deposited in the Protein Data Bank (accession code **6RPS**). Authors will release the atomic coordinates and experimental data upon article publication.

Acknowledgments

The authors thank Mr. Maurizio Amendola for his skillful technical assistance with X-ray measurements. This work was supported by a grant from Regione Campania PO FESR 2014–2020 "eMORFORAD."

Disclosure of interest

The authors declare that they have no conflict of interest.

Appendix A. Supplementary data

Supplementary data to this article can be found online at https://doi.org/10.1016/j.jmb.2019.10.022.

Received 1 July 2019;
Received in revised form 26 September 2019;
Accepted 17 October 2019
Available online xxxx

Keywords:
anticancer drugs;
carbonic anhydrase XII;
complex;
crystal structure;
monoclonal antibody

[†] These authors contributed equally to the work.

Abbreviations used:
hCAs, human carbonic anhydrases; P-GP, P-glycoprotein; Fab, antigen-binding fragment; AAZ, acetazolamide; mAb, monoclonal antibody.

References

[1] V. Alterio, A. Di Fiore, K. D'Ambrosio, C.T. Supuran, G. De Simone, Multiple binding modes of inhibitors to carbonic anhydrases: how to design specific drugs targeting 15 different isoforms? Chem. Rev. 112 (2012) 4421–4468.
[2] C.T. Supuran, G. De Simone (Eds.), Carbonic Anhydrases as Biocatalysts - from Theory to Medical and Industrial Applications, first ed. edit, Elsevier B. V, Amsterdam. The Netherlands, 2015.
[3] D.N. Silverman, R. McKenna, Solvent-mediated proton transfer in catalysis by carbonic anhydrase, Acc. Chem. Res. 40 (2007) 669–675.
[4] M. Aggarwal, B. Kondeti, C. Tu, C.M. Maupin, D.N. Silverman, R. McKenna, Structural insight into activity enhancement and inhibition of H64A carbonic anhydrase II by imidazoles, IUCrJ 1 (2014) 129–135.
[5] C.K. Tu, D.N. Silverman, C. Forsman, B.H. Jonsson, S. Lindskog, Role of histidine 64 in the catalytic mechanism of human carbonic anhydrase II studied with a site-specific mutant, Biochemistry 28 (1989) 7913–7918.
[6] M. Buonanno, A. Di Fiore, E. Langella, K. D'Ambrosio, C.T. Supuran, S.M. Monti, G. De Simone, The crystal

structure of a hCA VII variant provides insights into the molecular determinants responsible for its catalytic behavior, Int. J. Mol. Sci. 19 (2018) E1571, pii.
[7] S.K. Nair, D.W. Christianson, Structural properties of human carbonic anhydrase II at pH 9.5, Biochem.Biophys. Res. Commun. 181 (1991) 579–584.
[8] C.M. Maupin, N. Castillo, S. Taraphder, C. Tu, R. McKenna, D.N. Silverman, G.A. Voth, Chemical rescue of enzymes: proton transfer in mutants of human carbonic anhydrase II, J. Am. Chem. Soc. 133 (2011) 6223–6234.
[9] C.M. Maupin, G.A. Voth, Preferred orientations of His64 in human carbonic anhydrase II, Biochemistry 46 (2007) 2938–2947.
[10] B.S. Avvaru, C.U. Kim, K.H. Sippel, S.M. Gruner, M. Agbandje-McKenna, D.N. Silverman, R. McKenna, A short, strong hydrogen bond in the active site of human carbonic anhydrase II, Biochemistry 49 (2010) 249–251.
[11] S.Z. Fisher, C.M. Maupin, M. Budayova-Spano, L. Govindasamy, C. Tu, M. Agbandje-McKenna, D.N. Silverman, G.A. Voth, R. McKenna, Atomic crystal and molecular dynamics simulation structures of human carbonic anhydrase II: insights into the proton transfer mechanism, Biochemistry 46 (2007) 2930–2937.
[12] K. Hakansson, M. Carlsson, L.A. Svensson, A. Liljas, Structure of native and apo carbonic anhydrase II and structure of some of its anion-ligand complexes, J. Mol. Biol. 227 (1992) 1192–1204.
[13] Z. Fisher, J.A. Hernandez Prada, C. Tu, D. Duda, C. Yoshioka, H. An, L. Govindasamy, D.N. Silverman, R. McKenna, Structural and kinetic characterization of active-site histidine as a proton shuttle in catalysis by human carbonic anhydrase II, Biochemistry 44 (2005) 1097–1105.
[14] C.T. Supuran, V. Alterio, A. Di Fiore, D.A. K, F. Carta, S.M. Monti, G. De Simone, Inhibition of carbonic anhydrase IX targets primary tumors, metastases, and cancer stem cells: three for the price of one, Med. Res. Rev. 38 (2018) 1799–1836.
[15] S. Singh, C.L. Lomelino, M.Y. Mboge, S.C. Frost, R. McKenna, Cancer drug development of carbonic anhydrase inhibitors beyond the active site, Molecules 23 (2018) E1045, pii.
[16] S.M. Monti, C.T. Supuran, G. De Simone, Carbonic anhydrase IX as a target for designing novel anticancer drugs, Curr. Med. Chem. 19 (2012) 821–830.
[17] G. De Simone, V. Alterio, C.T. Supuran, Exploiting the hydrophobic and hydrophilic binding sites for designing carbonic anhydrase inhibitors, Expert Opin. Drug Discov. 8 (2013) 793–810.
[18] C.T. Supuran, Structure-based drug discovery of carbonic anhydrase inhibitors, J. Enzym. Inhib. Med. Chem. 27 (2012) 759–772.
[19] F. Pacchiano, F. Carta, P.C. McDonald, Y. Lou, D. Vullo, A. Scozzafava, S. Dedhar, C.T. Supuran, Ureido-substituted benzenesulfonamides potently inhibit carbonic anhydrase IX and show antimetastatic activity in a model of breast cancer metastasis, J. Med. Chem. 54 (2011) 1896–1902.
[20] Y. Lou, P.C. McDonald, A. Oloumi, S. Chia, C. Ostlund, A. Ahmadi, A. Kyle, U. Auf dem Keller, S. Leung, D. Huntsman, B. Clarke, B.W. Sutherland, D. Waterhouse, M. Bally, C. Roskelley, C.M. Overall, A. Minchinton, F. Pacchiano, F. Carta, A. Scozzafava, N. Touisni, J.Y. Winum, C.T. Supuran, S. Dedhar, Targeting tumor hypoxia: suppression of breast tumor growth and metastasis by novel carbonic anhydrase IX inhibitors, Cancer Res. 71 (2011) 3364–3376.
[21] C.R. Divgi, R.G. Uzzo, C. Gatsonis, R. Bartz, S. Treutner, J.Q. Yu, D. Chen, J.A. Carrasquillo, S. Larson, P. Bevan, P. Russo, Positron emission tomography/computed tomography identification of clear cell renal cell carcinoma: results from the REDECT trial, J. Clin. Oncol. 31 (2013) 187–194.
[22] ClinicalTrials.gov [Internet], Identifier NCT02215850, Safety Study of SLC-0111 in Subjects with Advanced Solid Tumours, National Library of Medicine (US), Bethesda (MD), 2014 Aug 11. Available from:https://clinicaltrials.gov/ct2/show/study/NCT02215850.
[23] K. Chamie, N.M. Donin, P. Klopfer, P. Bevan, B. Fall, O. Wilhelm, S. Storkel, J. Said, M. Gambla, R.E. Hawkins, G. Jankilevich, A. Kapoor, E. Kopyltsov, M. Staehler, K. Taari, A.J.A. Wainstein, A.J. Pantuck, A.S. Belldegrun, Adjuvant weekly girentuximab following nephrectomy for high-risk renal cell carcinoma: the ARISER randomized clinical trial, JAMA Oncol. 3 (2017) 913–920.
[24] O. Tureci, U. Sahin, E. Vollmar, S. Siemer, E. Gottert, G. Seitz, A.K. Parkkila, G.N. Shah, J.H. Grubb, M. Pfreundschuh, W.S. Sly, Human carbonic anhydrase XII: cDNA cloning, expression, and chromosomal localization of a carbonic anhydrase gene that is overexpressed in some renal cell cancers, Proc. Natl. Acad. Sci. U.S.A. 95 (1998) 7608–7613.
[25] D.A. Whittington, A. Waheed, B. Ulmasov, G.N. Shah, J.H. Grubb, W.S. Sly, D.W. Christianson, Crystal structure of the dimeric extracellular domain of human carbonic anhydrase XII, a bitopic membrane protein overexpressed in certain cancer tumor cells, Proc. Natl. Acad. Sci. U.S.A. 98 (2001) 9545–9550.
[26] C. Battke, E. Kremmer, J. Mysliwietz, G. Gondi, C. Dumitru, S. Brandau, S. Lang, D. Vullo, C. Supuran, R. Zeidler, Generation and characterization of the first inhibitory antibody targeting tumour-associated carbonic anhydrase XII, Cancer Immunol.Immunother. 60 (2011) 649–658.
[27] G. Gondi, J. Mysliwietz, A. Hulikova, J.P. Jen, P. Swietach, E. Kremmer, R. Zeidler, Antitumor efficacy of a monoclonal antibody that inhibits the activity of cancer-associated carbonic anhydrase XII, Cancer Res. 73 (2013) 6494–6503.
[28] B. von Neubeck, G. Gondi, C. Riganti, C. Pan, A. Parra Damas, H. Scherb, A. Erturk, R. Zeidler, An inhibitory antibody targeting carbonic anhydrase XII abrogates chemoresistance and significantly reduces lung metastases in an orthotopic breast cancer model in vivo, Int. J. Cancer 143 (2018) 2065–2075.
[29] P. Holliger, P.J. Hudson, Engineered antibody fragments and the rise of single domains, Nat. Biotechnol. 23 (2005) 1126–1136.
[30] A.L. Nelson, Antibody fragments: hope and hype, mAbs 2 (2010) 77–83.
[31] S.K. Gupta, P. Shukla, Microbial platform technology for recombinant antibody fragment production: a review, Crit. Rev. Microbiol. 43 (2017) 31–42.
[32] Y. Zhou, A.L. Goenaga, B.D. Harms, H. Zou, J. Lou, F. Conrad, G.P. Adams, B. Schoeberl, U.B. Nielsen, J.D. Marks, Impact of intrinsic affinity on functional binding and biological activity of EGFR antibodies, Mol. Cancer Ther. 11 (2012) 1467–1476.
[33] M.A. Proescholdt, C. Mayer, M. Kubitza, T. Schubert, S.Y. Liao, E.J. Stanbridge, S. Ivanov, E.H. Oldfield, A. Brawanski, M.J. Merrill, Expression of hypoxia-inducible

Please cite this article as: V. Alterio, M. Kellner, D. Esposito, et al., Biochemical and Structural Insights into Carbonic Anhydrase XII/Fab6A10 Complex, Journal of Molecular Biology, https://doi.org/10.1016/j.jmb.2019.10.022

carbonic anhydrases in brain tumors, Neuro Oncol. 7 (2005) 465–475.
[34] A. Zubriene, J. Smirnoviene, A. Smirnov, V. Morkunaite, V. Michailoviene, J. Jachno, V. Juozapaitiene, P. Norvaisas, E. Manakova, S. Grazulis, D. Matulis, Intrinsic thermodynamics of 4-substituted-2,3,5,6-tetrafluorobenzenesulfonamide binding to carbonic anhydrases by isothermal titration calorimetry, Biophys. Chem. 205 (2015) 51–65.
[35] E.W. Debler, R. Muller, D. Hilvert, I.A. Wilson, An aspartate and a water molecule mediate efficient acid-base catalysis in a tailored antibody pocket, Proc. Natl. Acad. Sci. U.S.A. 106 (2009) 18539–18544.
[36] C.T. Supuran, Carbonic anhydrases: novel therapeutic applications for inhibitors and activators, Nat. Rev. Drug Discov. 7 (2008) 168–181.
[37] V. Alterio, P. Pan, S. Parkkila, M. Buonanno, C.T. Supuran, S.M. Monti, G. De Simone, The structural comparison between membrane-associated human carbonic anhydrases provides insights into drug design of selective inhibitors, Biopolymers 101 (2014) 769–778.
[38] C.T. Supuran, How many carbonic anhydrase inhibition mechanisms exist? J. Enzym. Inhib. Med. Chem. 31 (2016).
[39] C.C. Wykoff, N. Beasley, P.H. Watson, L. Campo, S.K. Chia, R. English, J. Pastorek, W.S. Sly, P. Ratcliffe, A.L. Harris, Expression of the hypoxia-inducible and tumor-associated carbonic anhydrases in ductal carcinoma in situ of the breast, Am. J. Pathol. 158 (2001) 1011–1019.
[40] M.J. Hsieh, K.S. Chen, H.L. Chiou, Y.S. Hsieh, Carbonic anhydrase XII promotes invasion and migration ability of MDA-MB-231 breast cancer cells through the p38 MAPK signaling pathway, Eur. J. Cell Biol. 89 (2010) 598–606.
[41] A. Kivela, S. Parkkila, J. Saarnio, T.J. Karttunen, J. Kivela, A.K. Parkkila, A. Waheed, W.S. Sly, J.H. Grubb, G. Shah, O. Tureci, H. Rajaniemi, Expression of a novel transmembrane carbonic anhydrase isozyme XII in normal human gut and colorectal tumors, Am. J. Pathol. 156 (2000) 577–584.
[42] A.J. Kivela, S. Parkkila, J. Saarnio, T.J. Karttunen, J. Kivela, A.K. Parkkila, M. Bartosova, V. Mucha, M. Novak, A. Waheed, W.S. Sly, H. Rajaniemi, S. Pastorekova, J. Pastorek, Expression of von Hippel-Lindau tumor suppressor and tumor-associated carbonic anhydrases IX and XII in normal and neoplastic colorectal mucosa, World J. Gastroenterol. 11 (2005) 2616–2625.
[43] P. Hynninen, L. Vaskivuo, J. Saarnio, H. Haapasalo, J. Kivela, S. Pastorekova, J. Pastorek, A. Waheed, W.S. Sly, U. Puistola, S. Parkkila, Expression of transmembrane carbonic anhydrases IX and XII in ovarian tumours, Histopathology 49 (2006) 594–602.
[44] A.J. Kivela, S. Parkkila, J. Saarnio, T.J. Karttunen, J. Kivela, A.K. Parkkila, S. Pastorekova, J. Pastorek, A. Waheed, W.S. Sly, H. Rajaniemi, Expression of transmembrane carbonic anhydrase isoenzymes IX and XII in normal human pancreas and pancreatic tumours, Histochem. Cell Biol. 114 (2000) 197–204.
[45] J. Haapasalo, M. Hilvo, K. Nordfors, H. Haapasalo, S. Parkkila, A. Hyrskyluoto, I. Rantala, A. Waheed, W.S. Sly, S. Pastorekova, J. Pastorek, A.K. Parkkila, Identification of an alternatively spliced isoform of carbonic anhydrase XII in diffusely infiltrating astrocytic gliomas, Neuro Oncol. 10 (2008) 131–138.
[46] S.M. Monti, C.T. Supuran, G. De Simone, Anticancer carbonic anhydrase inhibitors: a patent review (2008 - 2013), Expert Opin. Ther. Pat. 23 (2013) 737–749.
[47] J. Chiche, K. Ilc, J. Laferriere, E. Trottier, F. Dayan, N.M. Mazure, M.C. Brahimi-Horn, J. Pouyssegur, Hypoxia-inducible carbonic anhydrase IX and XII promote tumor cell growth by counteracting acidosis through the regulation of the intracellular pH, Cancer Res. 69 (2009) 358–368.
[48] J. Doyen, S.K. Parks, S. Marcie, J. Pouyssegur, J. Chiche, Knock-down of hypoxia-induced carbonic anhydrases IX and XII radiosensitizes tumor cells by increasing intracellular acidosis, Front. Oncol. 2 (2013) 199.
[49] N. Lounnas, C. Rosilio, M. Nebout, D. Mary, E. Griessinger, Z. Neffati, J. Chiche, H. Spits, T.J. Hagenbeek, V. Asnafi, S.A. Poulsen, C.T. Supuran, J.F. Peyron, V. Imbert, Pharmacological inhibition of carbonic anhydrase XII interferes with cell proliferation and induces cell apoptosis in T-cell lymphomas, Cancer Lett. 333 (2013) 76–88.
[50] D. Gil, A.G. Schrum, Strategies to stabilize compact folding and minimize aggregation of antibody-based fragments, Adv. Biosci. Biotechnol. 4 (2013) 73–84.
[51] A. Maresca, C. Temperini, H. Vu, N.B. Pham, S.A. Poulsen, A. Scozzafava, R.J. Quinn, C.T. Supuran, Non-zinc mediated inhibition of carbonic anhydrases: coumarins are a new class of suicide inhibitors, J. Am. Chem. Soc. 131 (2009) 3057–3062.
[52] A. Maresca, C. Temperini, L. Pochet, B. Masereel, A. Scozzafava, C.T. Supuran, Deciphering the mechanism of carbonic anhydrase inhibition with coumarins and thiocoumarins, J. Med. Chem. 53 (2010) 335–344.
[53] K. D'Ambrosio, S. Carradori, S.M. Monti, M. Buonanno, D. Secci, D. Vullo, C.T. Supuran, G. De Simone, Out of the active site binding pocket for carbonic anhydrase inhibitors, Chem. Commun. 51 (2015) 302–305.
[54] M.T. Murri-Plesko, A. Hulikova, E. Oosterwijk, A.M. Scott, A. Zortea, A.L. Harris, G. Ritter, L. Old, S. Bauer, P. Swietach, C. Renner, Antibody inhibiting enzymatic activity of tumour-associated carbonic anhydrase isoform IX, Eur. J. Pharmacol. 657 (2011) 173–183.
[55] C. Xu, A. Lo, A. Yammanuru, A.S. Tallarico, K. Brady, A. Murakami, N. Barteneva, Q. Zhu, W.A. Marasco, Unique biological properties of catalytic domain directed human anti-CAIX antibodies discovered through phage-display technology, PLoS One 5 (2010), e9625.
[56] A. Yamaguchi, K. Usami, M. Shimabe, K. Hasegawa, M. Asada, K. Motoki, T. Tahara, K. Masuda, The novel CA IX inhibition antibody chKM4927 shows anti-tumor efficacy in vivo, Anticancer Res. 35 (2015) 1997–2004.
[57] D. Dekaminaviciute, V. Kairys, M. Zilnyte, V. Petrikaite, V. Jogaite, J. Matuliene, Z. Gudleviciene, D. Vullo, C.T. Supuran, A. Zvirbliene, Monoclonal antibodies raised against 167-180 aa sequence of human carbonic anhydrase XII inhibit its enzymatic activity, J. Enzym. Inhib. Med. Chem. 29 (2014) 804–810.
[58] F.W. Studier, Protein production by auto-induction in high density shaking cultures, Protein Expr.Purif. 41 (2005) 207–234.
[59] R.G. Khalifah, The carbon dioxide hydration activity of carbonic anhydrase. I. Stop-flow kinetic studies on the native human isoenzymes B and C, J. Biol. Chem. 246 (1971) 2561–2573.
[60] G. De Simone, A. Angeli, M. Bozdag, C.T. Supuran, J.Y. Winum, S.M. Monti, V. Alterio, Inhibition of carbonic anhydrases by a substrate analog: benzyl carbamate directly coordinates the catalytic zinc ion mimicking bicarbonate binding, Chem. Commun. 54 (2018) 10312–10315.

Please cite this article as: V. Alterio, M. Kellner, D. Esposito, et al., Biochemical and Structural Insights into Carbonic Anhydrase XII/Fab6A10 Complex, Journal of Molecular Biology, https://doi.org/10.1016/j.jmb.2019.10.022

[61] C.T. Supuran, A. Scozzafava, M.A. Ilies, F. Briganti, Carbonic anhydrase inhibitors: synthesis of sulfonamides incorporating 2,4,6-trisubstituted-pyridinium-ethylcarboxamido moieties possessing membrane-impermeability and in vivo selectivity for the membrane-bound (CA IV) versus the cytosolic (CA I and CA II) isozymes, J. Enzym. Inhib. 15 (2000) 381–401.

[62] M. Hilvo, L. Baranauskiene, A.M. Salzano, A. Scaloni, D. Matulis, A. Innocenti, A. Scozzafava, S.M. Monti, A. Di Fiore, G. De Simone, M. Lindfors, J. Janis, J. Valjakka, S. Pastorekova, J. Pastorek, M.S. Kulomaa, H.R. Nordlund, C.T. Supuran, S. Parkkila, Biochemical characterization of CA IX, one of the most active carbonic anhydrase isozymes, J. Biol. Chem. 283 (2008) 27799–27809.

[63] D. Vullo, M. Franchi, E. Gallori, J. Pastorek, A. Scozzafava, S. Pastorekova, C.T. Supuran, Carbonic anhydrase inhibitors: inhibition of the tumor-associated isozyme IX with aromatic and heterocyclic sulfonamides, Bioorg. Med. Chem. Lett 13 (2003) 1005–1009.

[64] K. D'Ambrosio, M. Lopez, N.A. Dathan, S. Ouahrani-Bettache, S. Kohler, G. Ascione, S.M. Monti, J.Y. Winum, G. De Simone, Structural basis for the rational design of new anti-Brucella agents: the crystal structure of the C366S mutant of L-histidinol dehydrogenase from Brucella suis, Biochimie 97 (2014) 114–120.

[65] G. Ascione, D. de Pascale, C. De Santi, C. Pedone, N.A. Dathan, S.M. Monti, Native expression and purification of hormone-sensitive lipase from Psychrobacter sp. TA144 enhances protein stability and activity, Biochem.Biophys. Res. Commun. 420 (2012) 542–546.

[66] Z. Otwinowski, W. Minor, Processing of X-ray diffraction data collected in oscillation mode, Methods Enzymol. 276 (1997) 307–326.

[67] J. Navaza, Amore - an automated package for molecular replacement, Acta Crystallogr. A 50 (1994) 157–163.

[68] A.T. Brunger, P.D. Adams, G.M. Clore, W.L. DeLano, P. Gros, R.W. Grosse-Kunstleve, J.S. Jiang, J. Kuszewski, M. Nilges, N.S. Pannu, R.J. Read, L.M. Rice, T. Simonson, G.L. Warren, Crystallography & NMR system: a new software suite for macromolecular structure determination, Acta Crystallogr. D Biol. Crystallogr. 54 (1998) 905–921.

[69] A.T. Brunger, Version 1.2 of the crystallography and NMR system, Nat. Protoc. 2 (2007) 2728–2733.

[70] G.N. Murshudov, P. Skubak, A.A. Lebedev, N.S. Pannu, R.A. Steiner, R.A. Nicholls, M.D. Winn, F. Long, A.A. Vagin, REFMAC5 for the refinement of macromolecular crystal structures, Acta Crystallogr. D Biol. Crystallogr. 67 (2011) 355–367.

[71] G.J. Kleywegt, T.A. Jones, xdlMAPMAN and xdlDATAMAN - programs for reformatting, analysis and manipulation of biomacromolecular electron-density maps and reflection data sets, Acta Crystallogr. D Biol. Crystallogr. 52 (1996) 826–828.

[72] T.A. Jones, J.Y. Zou, S.W. Cowan, M. Kjeldgaard, Improved methods for building protein models in electron density maps and the location of errors in these models, Acta Crystallogr. A: Found. Crystallogr. 47 (Pt 2) (1991) 110–119.

[73] E. Krissinel, K. Henrick, Inference of macromolecular assemblies from crystalline state, J. Mol. Biol. 372 (2007) 774–797.

Please cite this article as: V. Alterio, M. Kellner, D. Esposito, et al., Biochemical and Structural Insights into Carbonic Anhydrase XII/Fab6A10 Complex, Journal of Molecular Biology, https://doi.org/10.1016/j.jmb.2019.10.022